

Photoemission response of 2D electron states

V.N. Strocov

*Swiss Light Source, Paul Scherrer Institute, CH-5232 Villigen-PSI, Switzerland
(vladimir.strocov@psi.ch)*

A lucid Fourier analysis based description of the photoemission process is presented that directly relates photon energy ($h\nu$) dependent ARPES response of two-dimensional (2D) electron states to their wavefunctions. The states formed by quantum confinement of bulk Bloch waves (including Shockley-Tamm type surface and interface states, and quantum-well states) show periodic peaks of ARPES intensity as a function of $h\nu$. Amplitudes of these peaks reflect Fourier series of the oscillating Bloch-wave component of the wavefunction, and their broadening spatial confinement of its envelope function. In contrast, the 2D formed by local orbitals (dangling bonds and defects at the surface or interface) show aperiodic $h\nu$ -dependence, where the rate of decay reflects localization of these states in the out-of-plane direction. This formalism sets up a straightforward methodology to access fundamental properties of different 2D states, as illustrated by analysis of previous photoemission experimental data including the paradigm Al(100) surface state, quantum-well states in multilayer graphene and at the buried GaAlN/GaN interface, and molecular orbitals.

Keywords: Angle-resolved photoelectron spectroscopy (ARPES); electronic band structure and wavefunctions; quantum confinement; surface states; quantum-well states

Introduction

Two-dimensional (2D) electron states formed by quantum confinement (QC) play an important role in fundamental physics of solid-states systems and their device applications. One of numerous examples is the GaAlAs/GaAs interface where confinement of mobile electrons in a quantum-well (QW) formed by the interfacial band bending allowed realization of high electron mobility transistors (HEMTs) presently used in virtually all millimetre and microwave communication devices including cell phones (Mimura 2002). Such QW-states are formed by confinement of oscillating bulk Bloch waves whose out-of-plane periodicity is imposed by the periodic bulk potential $V(\mathbf{r})$ (for entries see (Chiang 2000 and Yoshimatsu *et al* 2011). Surface states of the Shockley-Tamm type is another example of electron states which can be viewed as resulting from QC, in this case between vacuum and a band gap in crystal bulk (Heine 1963, Inglesfield 1982). Their wavefunction is an evanescent Bloch wave whose periodic $B(z)$ -part is inherited from the bulk Bloch waves at the band gap edges (for theory of complex band structure see, for example, Heine 1963, Dederichs 1972 and Reuter 2017). Here, all such states formed by confinement of periodic bulk Bloch waves are treated on the same footing using a generalized terminology of *QC-type* states. The wavefunction of these states (sketched later on in Fig. 1) is represented by an oscillating Bloch wave, inherent in the periodic bulk $V(\mathbf{r})$, which is modulated by an envelope function describing the confinement. Another type of 2D states is local-orbital type (*LO-type*) states such as surface and interface states induced by dangling bonds or defects (Inglesfield 1982). Although the former can be delocalized in the in-plane direction and the latter not, common to all such states is that they are localized in the out-of-plane direction and not connected with confinement of bulk states, with their wavefunction (also sketched in Fig. 1) essentially reduced to the aperiodic envelope function. As we will see here, the presence or absence of the oscillating wavefunction component causes totally different photoemission response of these two types of 2D states.

Angle-resolved photoelectron spectroscopy (ARPES) is the unique experimental method that allows explore of electron states with resolution in their binding energy E_b and momentum \mathbf{k} (see, for example, the recent review by Suga & Tuschke 2015). Surface states have in the past been one of the most popular applications of ARPES in the VUV photon energy range ($h\nu < 100$ eV) where the electron mean free path λ , defining the probing depth of this technique, is of the order of 0.5 nm (Powell *et al* 1999). \mathbf{k} -resolved studies of electron states at buried interfaces have however become accessible only with advent ARPES in the soft-X-ray range ($h\nu$ typically from 300 to 1500 eV) where increase of photoelectron kinetic energy E_k boosts λ by a factor of 3-5 (Strocov *et al* 2014, Cancellieri *et al* 2016).

Owing to 2D character of all surface and interface states, their ARPES response shows spectral peaks whose E_b is independent of out-of-plane photoelectron momentum K_z varied in the ARPES experiment through $h\nu$. Characteristic of the QC-type states is however that the corresponding ARPES intensity periodically oscillates as a function of K_z . First noted in the pioneering work of Louie *et al* (1980) on the Cu(111) surface state, this phenomenon was later studied experimentally and theoretically for a number of QC-systems including metal thin films (Ortega *et al* 1993, Mugarza *et al* 2001, Chiang *et al* 2000), multilayer graphene (Ohta *et al* 2007), buried delta-layers [Miwa *et al* 2013] and various surface states (Kevan *et al* 1985, Hofmann *et al* 2004, Krasovskii *et al* 2008, Borghetti *et al* 2012). The LO-type states, in contrast, show an aperiodic ARPES response decaying with K_z .

Following the previous works [Louie *et al* 1980, Kevan *et al* 1985], a lucid formalism is developed here that directly relates the ARPES intensity oscillations to Fourier series and spatial confinement of the 2D states, and can therefore be used for their experimental determination. Of crucial importance for this purpose is the use of high excitation energies whereby the ARPES final states become pure plane waves without their hybridization (Strocov *et al* 2012). This formalism is illustrated in application to previous photoemission experimental data on the Al(100) surface (Hofmann *et al* 2004).

Fourier-transform formalism of ARPES

Within the one-step theory of photoemission – see, for example, Feibelman & Eastman (1974) – the ARPES intensity is found as $I_{PE} \propto |\langle f | \mathbf{A} \cdot \mathbf{p} | i \rangle|^2$, where $\langle f |$ is the final state described as the time-reversed LEED state and $| i \rangle$ the initial state, which are coupled through the vector potential \mathbf{A} of incident electromagnetic field and momentum operator \mathbf{p} . Neglecting the explicit matrix element effects embedding the experimental geometry (see, for example, Moser 2017), this expression can be simplified to the scalar product of $\langle f |$ and $| i \rangle$, $I_{PE} \propto |\langle f | i \rangle|^2$. We here assume that the final-state momentum \mathbf{K} is corrected back to the initial-state one \mathbf{k} for the photon momentum $p = h\nu/c$ which is significant in the soft-X-ray range.

For sufficiently high excitation energy $h\nu$, when E_k much exceeds the $V(\mathbf{r})$ corrugation, the free-electron (FE) approximation usually holds for the final states which can in this case be represented by a plane wave $e^{i\mathbf{K}\mathbf{r}}$ periodic in the in-plane direction \mathbf{r}_{xy} and damped in the out-of-plane one z (non-FE effects in the final states, which can be particularly strong at low excitation energies $h\nu$ – see Strocov *et al* (2006) and references therein – will be discussed later). Introducing out-of-plane damping of final state due to incoherent scattering processes, $\langle f |$ can be represented as $\langle f | \propto e^{i\mathbf{K}_{xy}\mathbf{r}_{xy}} e^{iK_z z}$, where K_z is complex, with its real part K_z^r describing the oscillating z -dependent part of the $\langle f |$ -wavefunction and imaginary part K_z^i its damping into the sample depth due to finite photoelectron mean free path $\lambda = 1/2K_z^i$ (the factor 2 comes from squaring of the wavefunction amplitude for electron density), $\langle f | \propto e^{i\mathbf{K}_{xy}\mathbf{r}_{xy}} e^{iK_z^r z} e^{-K_z^i z}$. In turn, $| i \rangle$ also obeys the in-plane periodicity, and can be expanded over 2D reciprocal vectors \mathbf{g} as $| i \rangle = \sum_{\mathbf{g}} A_{\mathbf{k}_{xy}+\mathbf{g}}(z) e^{i(\mathbf{k}_{xy}+\mathbf{g})\mathbf{r}_{xy}}$, where \mathbf{k}_{xy} is the in-plane electron momentum in the reduced BZ and coefficients $A_{\mathbf{k}_{xy}+\mathbf{g}}(z)$ represent the $| i \rangle$ -wavefunction behavior in the z -direction, being periodic for 3D states and confined for 2D states. Orthogonality of the in-plane propagating plane waves in the above expansions for $\langle f |$ and $| i \rangle$ implies that the only term in $| i \rangle$ giving non-zero contribution to $\langle f | i \rangle$ satisfies the condition $\mathbf{k}_{xy} + \mathbf{g} = \mathbf{K}_{xy}$ i.e. the above sum over \mathbf{g} reduces to $| i \rangle = A_{\mathbf{K}_{xy}}(z) e^{i\mathbf{K}_{xy}\mathbf{r}_{xy}}$.

With the above expansions of $\langle f |$ and $| i \rangle$, I_{PE} as a function of \mathbf{K}_{xy} becomes $I_{PE}(\mathbf{K}_{xy}) \propto \left| \langle e^{i\mathbf{K}_{xy}\mathbf{r}_{xy}} e^{iK_z^r z} e^{-K_z^i z} | A_{\mathbf{K}_{xy}}(z) e^{i\mathbf{K}_{xy}\mathbf{r}_{xy}} \rangle \right|^2 = \left| \langle e^{iK_z^r z} e^{-K_z^i z} | A_{\mathbf{K}_{xy}}(z) \rangle \right|^2$. Being proportional to $|A_{\mathbf{K}_{xy}}|^2$, the

\mathbf{K}_{xy} -dependent I_{PE} reflects essentially the 2D Fourier series of the $|i\rangle$ -states periodic in the out-of-plane spatial coordinates.

Transferring the damping $e^{-K_z^i z}$ into the $|i\rangle$ -part, we obtain $I_{PE}^{\mathbf{K}_{xy}} \propto \left| \left\langle e^{iK_z^i z} \left| e^{-K_z^i z} A_{\mathbf{K}_{xy}}(z) \right\rangle \right|^2$. In the explicit form, this expression reads as $I_{PE}^{\mathbf{K}_{xy}}(K_z) \propto \left| \int_0^\infty e^{iK_z^i z} \left\{ e^{-K_z^i z} A_{\mathbf{K}_{xy}}(z) \right\} dz \right|^2$, where the lower integration limit implies that the $|i\rangle$ -wavefunction terminates at the surface $z=0$. Physically, this formula shows that the K_z -dependent I_{PE} for given photoelectron \mathbf{K}_{xy} is simply the squared FT

$$I_{PE}^{\mathbf{K}_{xy}}(K_z) \propto \left| F_{K_z} \left\{ e^{-K_z^i z} A_{\mathbf{K}_{xy}}(z) \right\} \right|^2 \quad (1)$$

of the (final-state damping weighted) z -dependent coefficient $A(z)$ for this \mathbf{K}_{xy} in 2D expansion of the $|i\rangle$ -wavefunction. This property of the ARPES response can in principle be used to reconstruct the wavefunctions of 2D states using iterative algorithms similar to those used in molecular wavefunction reconstruction (Puschnig *et al* 2009, Weiss *et al* 2015, Bradshaw & Woodruff 2015, Kliuiev *et al* 2016). If λ is much larger than the $|i\rangle$ -wavefunction localization region, a likely situation for sufficiently high $h\nu$, the above FT simplifies to $I_{PE}^{\mathbf{K}_{xy}}(K_z) \propto \left| F_{K_z} \left\{ A_{\mathbf{K}_{xy}}(z) \right\} \right|^2$. We note that whereas the \mathbf{K}_{xy} -dependence of I_{PE} is represented by the Fourier series, whose discrete character reflects the in-plane periodicity of the system, its K_z -dependence is represented by the integral Fourier transform, whose continuous character reflects the out-of-plane aperiodicity.

We will now focus on the 2D states that are confined in the out-of-plane direction. For the QC-type states sketched in Fig. 1 (a), the coefficients $A_{\mathbf{K}_{xy}}(z)$ representing the $|i\rangle$ -wavefunction for given \mathbf{K}_{xy} can be written as a slowly varying envelope function $E(z)$ that modulates a Bloch wave $B_{\mathbf{K}_{xy}}(z)$ which is derived from the periodic bulk $V(\mathbf{r})$, periodic in the out-of-plane direction and characterized by certain momentum k_z (Ortega *et al* 1996, Chiang 2000, Mugarza *et al* 2001)

$$A_{\mathbf{K}_{xy}}(z) = E(z) \cdot B_{\mathbf{K}_{xy}}(z) \quad (2)$$

We note that the $E(z)$ -functions can be described analytically by Airy functions, if $V(z)$ confining the QC-type states is approximated by a triangular shape, and by Bessel functions if a more appropriate exponential approximation $V(z) \propto -V_0 e^{-2z/a}$ is used, where V_0 is the characteristic depth and a width of $V(z)$ (Jovic *et al* 2017, Moser *et al* 2018). The $B(z)$ -functions, strictly speaking, are standing waves including two Bloch waves with $\pm k_z$ propagating in opposite out-of-plane directions, however, for brevity of the formalism we keep here only one of them. The same expression (2) applies to the LO-type states also sketched in Fig. 1 (b), and in that case $A_{\mathbf{K}_{xy}}(z)$ reduces to $E(z)$, with $B_{\mathbf{K}_{xy}}(z) = B_{\mathbf{K}_{xy}}$ remaining merely a constant depending on \mathbf{K}_{xy} .

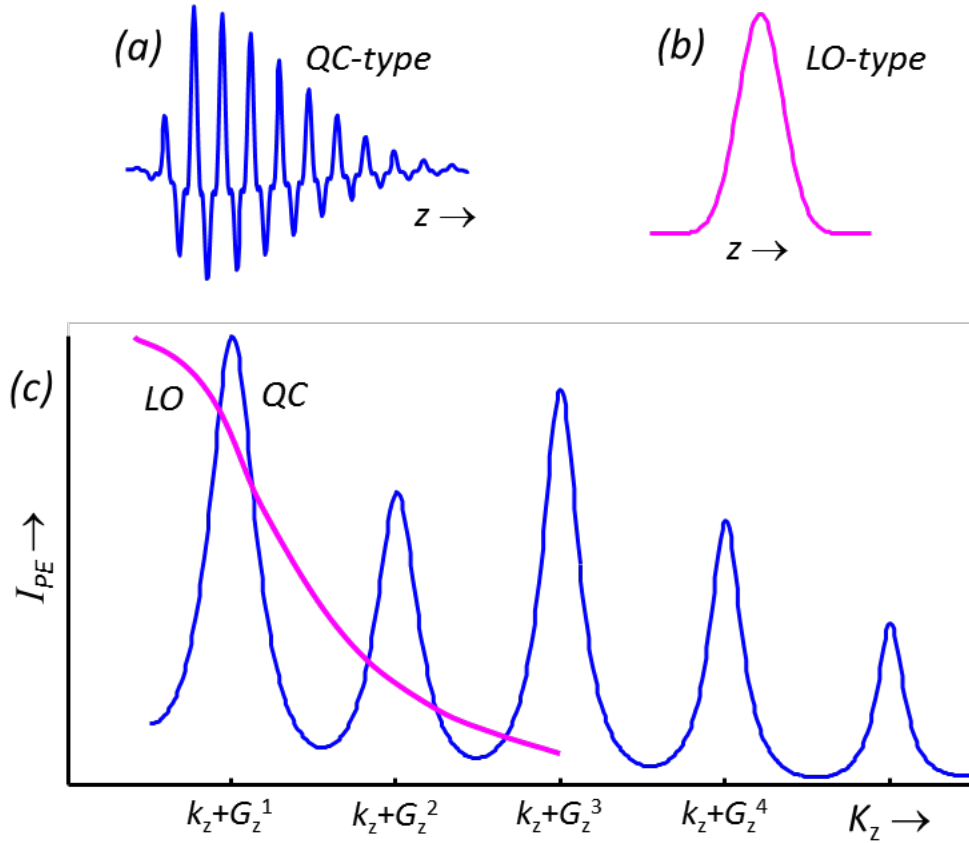


Fig. 1. Schematic wavefunctions of the QC-type (a) and LO-type (b), and the corresponding pattern of their ARPES response $I_{PE}(K_z)$ (c). Due to the higher harmonics in the Bloch-wave part of the QC-type states, their ARPES response is characterized by G_z -periodic peaks whose amplitudes reflect Fourier series of the periodic Bloch-wave part of these states, and widths their spatial extension combined with the photoelectron λ . In contrast, the LO-type states are characterized by an aperiodic decay of $I_{PE}(K_z)$. In any case the $I_{PE}(K_z)$ -dependences vary with \mathbf{K}_{xy} .

In general case, the $B_{\mathbf{K}_{xy}}(z)$ adapted to the periodic $V(\mathbf{r})$ can be expanded in a Fourier series over out-of-plane reciprocal vectors G_z of the host 3D lattice as $B_{\mathbf{K}_{xy}}(z) = \sum_{G_z} C_{\mathbf{K}_{xy}}^{G_z} e^{i(k_z + G_z)z}$. Assembling all

terms in the above expression (1) for the photocurrent $I_{PE}^{\mathbf{K}_{xy}}(K_z)$, we arrive at $I_{PE}^{\mathbf{K}_{xy}}(K_z) \propto$

$$\left| F_{K_z} \left\{ e^{-K_z^i z} \cdot E(z) \cdot \sum_{G_z} C_{\mathbf{K}_{xy}}^{G_z} e^{i(k_z + G_z)z} \right\} \right|^2 = \left| \sum_{G_z} C_{\mathbf{K}_{xy}}^{G_z} F_{K_z} \left\{ e^{-K_z^i z} \cdot E(z) \cdot e^{i(k_z + G_z)z} \right\} \right|^2 =$$

$$\left| \sum_{G_z} C_{\mathbf{K}_{xy}}^{G_z} F_{K_z} \left\{ e^{-K_z^i z} \cdot E(z) \right\} * F_{K_z} \left\{ e^{i(k_z + G_z)z} \right\} \right|^2, \text{ where the FT is broken down in convolution of two}$$

transforms. As $F_{K_z} \left\{ e^{i(k_z + G_z)z} \right\}$ equals simply to the δ -function $\delta(K_z - (k_z + G_z))$, this yields

$$I_{PE}^{\mathbf{K}_{xy}}(K_z) \propto \left| \sum_{G_z} C_{\mathbf{K}_{xy}}^{G_z} F_{K_z} \left\{ e^{-K_z^i z} \cdot E(z) \right\} * \delta(K_z - (k_z + G_z)) \right|^2. \text{ Using the } \delta\text{-function convolution rule}$$

$f(x) * \delta(x-a) = f(x-a)$, we obtain the following expression for the K_z -dependent ARPES response $I_{PE}(K_z)$ of 2D states:

$$I_{PE}^{\mathbf{K}_{xy}}(K_z) \propto \left| \sum_{G_z} C_{\mathbf{K}_{xy}}^{G_z} F_{K_z - (k_z + G_z)} \left\{ e^{-K_z^i z} \cdot E(z) \right\} \right|^2 \quad (3)$$

Inside the squared absolute value, this expression sums up over a series of functions $F_{K_z - (k_z + G_z)} \left\{ e^{-K_z^i z} \cdot E(z) \right\}$. As the $\langle f|$ - and 2D $|i\rangle$ -wavefunctions both decay with z , these functions are in general peaks centered at $k_z + G_z$ which decay with detuning of K_z from the peak center.

Essential for the validity of this straightforward connection between the ARPES response and Fourier composition of the $|i\rangle$ -states is that the final states have the FE-character, i.e. described by a pure plane wave $e^{i\mathbf{K}\mathbf{r}}$. Otherwise, these states are a mixture of plane waves $\sum_{\mathbf{K}} A_{\mathbf{K}} e^{i\mathbf{K}\mathbf{r}}$ extending over \mathbf{K}

with different \mathbf{K}_{xy} and K_z projections. In this case $I_{PE}^{\mathbf{K}_{xy}}(K_z)$ would mix up the corresponding Fourier components of the $|i\rangle$ -state, rendering interpretation of the experimental data ambiguous. In general, high $h\nu$ much exceeding the atomic corrugation of $V(\mathbf{r})$ are required to ensure purely FE-character of the final states (Strocov *et al* 2012).

The above lucid description of the ARPES process obviously neglects the experimental geometry and photon polarization effects as well as non-FE effects in the final states important for quantitative description of the ARPES intensity. They are correctly taken into account by the one-step photoemission theory within its Bloch-wave or scattering theory formulations, for entries relevant for the 2D states see Krasovskii & Schattke 2004, Krasovskii *et al* 2008, and Braun & Donath 2004, respectively. The heavy computational machinery of these first-principles methods obscures however the Fourier composition roots of the ARPES intensity behavior.

Characteristic ARPES response patterns

QC-states

The QC-type states, sketched in Fig. 1 (a), typically have a long-range character expressed by relatively large extension of their $E(z)$. If the final-state extension is also relatively large as expressed by small K_z^i , which is typical of high E_k , the peaks of the $F_{K_z - (k_z + G_z)} \left\{ e^{-K_z^i z} \cdot E(z) \right\}$ functions in the above expression (3) for ARPES intensity do not overlap in K_z . In this case the squared absolute value can be exchanged with the sum as

$$I_{PE}^{\mathbf{K}_{xy}}(K_z) \propto \sum_{G_z} \left| C_{\mathbf{K}_{xy}}^{G_z} \right|^2 \left| F_{K_z - (k_z + G_z)} \left\{ e^{-K_z^i z} \cdot E(z) \right\} \right|^2. \quad (4)$$

This formula contains the key mathematical message of this work: K_z -dependent ARPES response of the QC-states appears as a sequence of G_z -periodic peaks weighted by the Fourier series amplitudes

of the underlying Bloch wave. This characteristic pattern is sketched in Fig. 1 (c). We should highlight its three important aspects:

(1) The peaks are centered at the K_z -values equal to the $k_z + G_z$ vectors of the Fourier series of the periodic $B(z)$ -part of the QC-wavefunction (Louie *et al* 1980, Ortega *et al* 1993, Mugarza *et al* 2000). This fact is a manifestation of the periodic Bloch wave origin of the QC-state. Physically, whenever K_z of the $\langle f|$ -wavefunction hits some $k_z + G_z$ harmonic of the $|i\rangle$ -one, the ARPES intensity blows up. In the reduced Brillouin zone picture, this condition is equivalent to the out-of-plane momentum conservation $K_z = k_z$ (vertical transitions) between the $\langle f|$ - and $|i\rangle$ -states.

As a minor refinement to this picture, we recall that the standing-wave-like QC-type states in principle include two Bloch waves with opposite signs of k_z , splitting each $I_{PE}(K_z)$ peak into two ones separated by $2|k_z|$, but this separation is usually much smaller than G_z . Furthermore, we note that the theoretical approaches which reduce the QC-type states to merely $E(z)$ -functions neglecting the periodic $B(z)$ -parts (Jovic *et al* 2017, Moser *et al* 2018) are unable to reproduce the characteristic K_z -periodicity of I_{PE} . Our formalism reduces to these approaches by retaining in the sum (4) only one non-zero $C_{\mathbf{K}_{xy}}^{G_z}$ coefficient at $G_z = 0$.

(2) The peak amplitudes are proportional to $\left|C_{\mathbf{K}_{xy}}^{G_z}\right|^2$ defined by the Fourier-series coefficients of the $B(z)$ -functions. Therefore, the K_z -dependent ARPES intensity informs the Fourier series of the periodic Bloch-wave content of the QC-wavefunction.

Furthermore, we note that the peak values at $K_z = k_z + G_z$ are all proportional to $\left|F_0\left\{e^{-K_z^i z} \cdot E(z)\right\}\right|^2$ or, in the explicit form, to $\left|\int_0^\infty e^{-K_z^i z} E(z) dz\right|^2$. This means that the ARPES signal scales up with spatial extension of both $\langle f|$ - and $|i\rangle$ -states into the crystal interior. The $I_{PE}(K_z)$ -dependences vary with \mathbf{K}_{xy} through the $\left|C_{\mathbf{K}_{xy}}^{G_z}\right|^2$ coefficients.

(3) The peaks have the shape defined by FT of the $E(z)$ envelope function of the $|i\rangle$ -states weighted with the final-state decay $e^{-K_z^i z}$. With the former being the same for all peaks, the peak shape will however depend on K_z through the $\lambda(E_k)$ dependence. Therefore, K_z -broadening of the ARPES peaks informs the $E(z)$ -function of the 2D valence electron states. The correct shape of the $I_{PE}(K_z)$ peaks is reproduced even theoretical approaches neglecting the periodic $B(z)$ -content of the QC-wavefunctions (Jovic *et al* 2017, Moser *et al* 2018).

Unfolding the last point, we note that in many cases, in particular for the surface states, $E(z)$ can be approximated by exponent e^{-Dz} , where D is the decay constant connected with the attenuation length d as $D=1/2d$ (the factor 2 comes from squaring of the wavefunction amplitude for electron

density). Combining it with the final-state damping $e^{-K_z^i z}$, we obtain $\left| F_{K_z-(k_z+G_z)} \left\{ e^{-K_z^i z} \cdot E(z) \right\} \right|^2 = \left| F_{K_z-(k_z+G_z)} \left\{ e^{-(K_z^i+D)z} \right\} \right|^2$. The latter is a Lorentzian $\left(1 + \left(\frac{K_z - (k_z + G_z)}{K_z^i + D} \right)^2 \right)^{-1}$ having full width at half maximum (FWHM) equal to $\Delta = 2(K_z^i + D)$ (E_k -dependence of $K_z^i = 1/2\lambda$ over the peak width can be neglected). In terms of attenuation length, the obtained FWHM is

$$\Delta = \lambda^{-1} + d^{-1} \quad (5)$$

Therefore, with a good estimate of photoelectron λ for given E_k , Lorentzian FWHM of an experimental $I_{PE}(K_z)$ -peak directly informs spatial extension of the QC-state. Under the condition $\lambda \gg d$, which might be achieved at sufficiently high $h\nu$, the FWHM will be simply equal to d^{-1} . We note that the QC-wavefunctions described by Bessel functions in exponential $V(z)$ deliver the ARPES peaks somewhat different in shape and width (Jovic *et al* 2017, Moser *et al* 2018) compared to the above e^{-Dz} wavefunctions.

We note that the above FT-based formalism puts on rigorous grounds and generalizes similar earlier theories to describe ARPES of surface states (Louie *et al* 1980, Kevan *et al* 1985). We note that often the QC-states are described within a simplified phase accumulation model that essentially replaces the sharply oscillating Bloch waves by smooth plane waves (see, for example, the review by Milun *et al* 2002) or simply reducing them to solely the $E(z)$ -function confined in one-dimensional $V(z)$ (Mooser *et al* 2018 and references). In a sense, this reminds the idea of pseudopotential where the real sharply oscillating wavefunction is replaced by its smooth pseudo-wavefunction analogue. Similarly, the phase accumulation model is only relevant for the energy levels and $E(z)$ -functions. However, neglecting the effects embedded in the periodic $B(z)$ -functions, this model is unable to correctly reproduce the characteristic periodic ARPES response of the QC-states.

LO-states

We will now turn to another type of 2D states, the LO-type ones, which have purely surface or interface origin and are unrelated to any bulk Bloch waves. Schematically shown in Fig. 1 (b), such out-of-plane localized states can be formed, for example, by dangling bonds on semiconductor surfaces (Inglesfield 1982) or by surface and interface defect states. $I_{PE}(K_z)$ -dependence for such states follows a pattern totally different from the above QC-states. In this case the sum over G_z in the above expression (3) for ARPES intensity retains the sole term

$$I_{PE}^{\mathbf{K}_{xy}}(K_z) \propto \left| B_{\mathbf{K}_{xy}} \right|^2 \left| F_{K_z} \left\{ e^{-K_z^i z} \cdot E(z) \right\} \right|^2, \quad (6)$$

where $C_{\mathbf{K}_{xy}}^{G_z=0}$ is replaced back by the \mathbf{K}_{xy} -dependent constant $B_{\mathbf{K}_{xy}}$ from the expression (2). Essentially, ARPES response of the LO-type states is reduced to merely the first $G_z = 0$ peak of the $I_{PE}(K_z)$ dependence (3).

In contrast to the QC-type states, such $I_{PE}(K_z)$ -dependence is aperiodic and, as $E(z)$ is typically smooth and dominated by low spatial frequencies, rapidly decays with K_z as sketched in Fig. 1 (c). This characteristic ARPES response of the LO-type states sharply contrasts to the periodic and slowly decaying ARPES response of the QC-type states. We note that in the LO-case the $I_{PE}(K_z)$ dependence varies with \mathbf{K}_{xy} through the coefficients $B_{\mathbf{K}_{xy}}$.

If wavefunctions of the LO-states are symmetric in the out-of-plane direction like the s- or p_{xy} -orbitals, in many cases their $E(z)$ can be approximated by a Gaussian $e^{-2\ln 2 \left(\frac{z}{d}\right)^2}$ where d is FWHM of corresponding electron density distribution (mind the factor 2 coming from the wavefunction squaring). Combining it with the final-state damping $e^{-K_z^i z}$, for any \mathbf{K}_{xy} we obtain

$$I_{PE}^{\mathbf{K}_{xy}}(K_z) \propto \left| F_{K_z} \left\{ e^{-K_z^i z} \cdot e^{-2\ln 2 \left(\frac{z}{d}\right)^2} \right\} \right|^2 = \left(1 + \left(\frac{K_z}{K_z^i} \right)^2 \right)^{-1} * e^{-\frac{d^2}{8\ln 2} K_z^2} \text{ which is a convolution of Lorentzian}$$

(distorted by the K_z -dependence of K_z^i) and Gaussian profiles centered at $K_z = 0$. Physically, the smaller λ and d in these profiles, the faster the decay of this ARPES intensity with $h\nu$. With a good estimate of photoelectron $\lambda(E)$, fitting of the experimental K_z -dependence with this profile will yield an estimate of the wavefunction spatial extension d . If we can neglect the K_z -dependence of K_z^i through the Lorentzian profile, $I_{PE}(K_z)$ reduces to a Voigt profile with its FWHM approximated as

$$0.53K_z^i + \sqrt{0.22(K_z^i)^2 + \left(\frac{4\sqrt{2\ln 2}}{d} \right)^2}. \text{ Accuracy of this approximation improves with decrease of } d$$

towards $d \ll \lambda$, when the Lorentzian component with less certain K_z^i becomes negligible. We note that whereas these formulas, based on Gaussian approximation of the out-of-plane symmetric LO-wavefunctions, predict the increase of $I_{PE}(K_z)$ towards $K_z = 0$, for the antisymmetric wavefunctions like the p_z -orbitals the corresponding $I_{PE}(K_z)$ goes there to zero (Weiss *et al* 2015). In any case, however, $I_{PE}(K_z)$ is aperiodic and decays with increase of K_z .

Analysis of experimental ARPES data

QC-states

Belonging to the QC-type states are the Shockley-Tamm surface states which are essentially bulk Bloch waves, confined at the surface by band gaps in the bulk band structure. Owing to the higher Fourier components of the Bloch waves and typically long-range character of these surface states, the oscillating ARPES signal from them can persist with increase of $h\nu$ up to 1 keV and even higher. This can be illustrated by results of Hofmann *et al* (2002) on the Shockley-Tamm surface state on Al(100) which are reproduced in Fig. 2. The ARPES peaks coming from the bulk sp -band disperse as a function of K_z varied through $h\nu$. The dispersion maxima at three consecutive $h\nu$ -values are achieved where K_z reaches the X-point. The surface state peak (marked SS) in the sp -band gap, in contrast, does not disperse as a function of K_z that is characteristic of its 2D nature. However, its intensity

blows up whenever K_z reaches the X-point, following the periodic $I_{PE}(K_z)$ pattern in Fig. 1 (c). This indicates that k_z of the periodic $B(z)$ -part of the surface state wavefunction falls onto the X-point. Even at high $h\nu$ the ARPES response of the surface state stays comparable with that of the bulk states, which is consistent with its large out-of-plane extension of $>10 \text{ \AA}$. However, a quantitative evaluation of $E(z)$ from these data is difficult because energy resolution of this early soft-X-ray ARPES experiment was insufficient to resolve the surface state peak from the sp -bands in the X-point. Another example of strong oscillating ARPES response persisting at high $h\nu$ is the surface state in BiTeI (Landolt *et al* 2013).

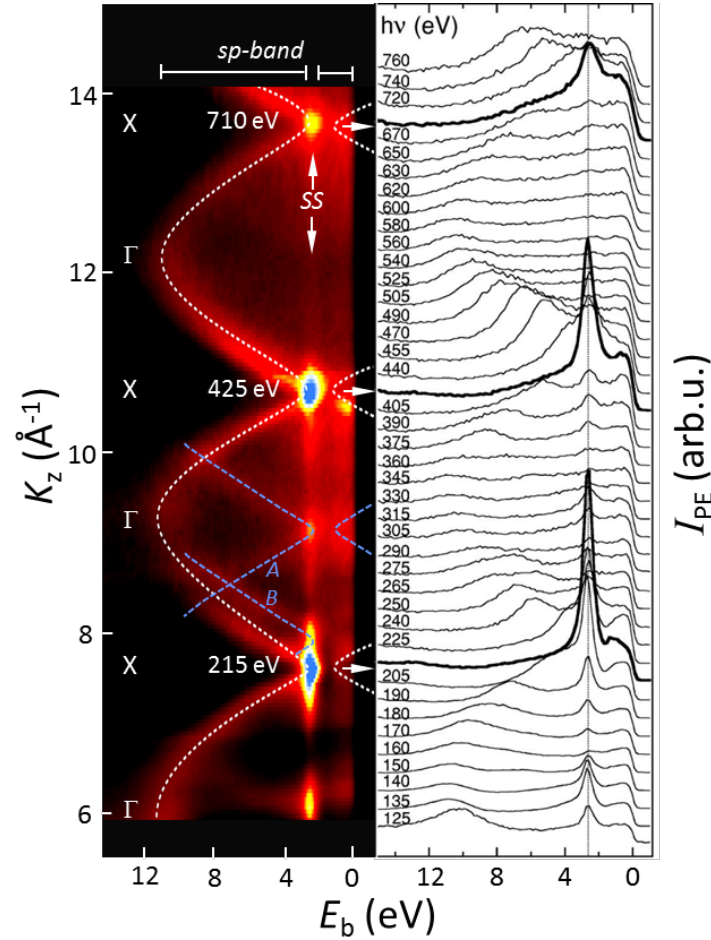


Fig. 2. ARPES data on Al(100) in a wide $h\nu$ -range. The ARPES peaks oscillating in E_b as a function of $h\nu$ manifest the bulk sp -bands, and those at constant E_b the surface state (SS). In agreement with the characteristic pattern in Fig. 1, its response blows up whenever K_z comes to the X-point. The secondary dispersion branches A and B of the sp -bands manifest multiband composition of the final states (adapted from Hofmann *et al* 2002).

An intriguing peculiarity of the data on Al(100) is that apart from the main dispersion branch of the bulk ARPES peaks one can observe few weaker secondary branches (marked A-B) that correspond to different k_z -values. In particular, $h\nu \sim 330 \text{ eV}$ brings k_z of the main branch to the Γ -point and that of the branch A to X. This fact evidences that in this case the final state deviates from the FE-type plane wave $e^{i\mathbf{K}\mathbf{r}}$ that would have selected one single k_z . In fact, it incorporates two different bands with different k_z and leading Fourier components $e^{i(k_z+G_z)z}$ which produce ARPES peaks of similar

intensity. One may think of such multiband final-state as a composition of umklapp bands or, in the Mahan's terminology, secondary photoemission cones (Mahan 1970). This phenomenon beyond the simple FE-approximation, resulting from hybridization of plane waves through $V(\mathbf{r})$, has been studied experimentally and theoretically in low-energy ARPES for bulk bands of various materials including Cu (Strocov *et al* 1997) and transition metal dichalcogenides (Strocov *et al* 1997, Strocov *et al* 2006, Krasovskii *et al* 2007) as well as surface states, in particular for the Al(100) and (111) surfaces (Krasovskii *et al* 2008). It is surprising to see in Fig. 2 that, although Al is one of the most FE-materials, the multiband final-state composition carries on at least to 400 eV. This phenomenon is actually surprisingly common in the soft-X-ray energy range, and will be addressed in detail elsewhere. Here we only note that it does not in general hamper interpretation of soft-X-ray ARPES data, because the intrinsic out-of-plane momentum broadening Δk_z (Strocov 2003) in this $h\nu$ -range typically reduces below k_z -separation of different Bloch waves that allows reliable assignment of the corresponding spectral structures. Non-FE effects in ARPES of molecular systems are discussed below.

Further examples of $h\nu$ -dependent ARPES of surface states, starting from the pioneering work of Louie *et al* (1980) on Cu(111), include various surfaces of Al, Cu, Ag and Au (Kevan *et al* 1985, Krasovskii *et al* 2008, Borghetti *et al* 2012), topological materials (Bianchi *et al* 2010), Weil semimetals (Jiang *et al* 2017), etc.

For the QW-states, an impressive example of their periodic ARPES response has been demonstrated for thin Ag films on Ni(111) (Miller *et al* 1994) where constant-initial-state spectral peaks from the states confined in Ag exposed a clear cyclic behaviour of their intensity. Another example is thin Cu(100) films on Co(100) (Mugarza *et al* 2000, Mugarza *et al* 2001). In agreement with the pattern in Fig. 1, the ARPES peaks have been found at $h\nu$ -values corresponding to vertical transitions between the initial-state k_z and final-state K_z . Furthermore, this study has identified a multiband final-state composition at the Cu(100) surface going up to 100 eV (Strocov *et al* 1997, Mugarza *et al* 2001). Another study of QW-states formed in Cu films on Co(100) and Co(110) (Hansen *et al* 1997) has shown that modulations of their $h\nu$ -dependent $I_{PE}(h\nu)$ are related by k_z conservation to dispersion of the Cu bulk sp -band that these QW-states are derived from, in agreement with our FT-based theory. Semiconductor surfaces can also bear QW-states formed from bulk CB states confined in the surface band-bending $V(\mathbf{r})$. A recent example is InN where the band bending can be tuned, for example, by absorption of potassium (Colakerol *et al* 2015) or water (Jovic *et al* 2017). These QW-states demonstrate the same periodic ARPES response pattern (Jovic *et al* 2017). We note that at sufficiently low E_k the QW can also confine the $\langle f|$ -wavefunctions just as the $|i\rangle$ -ones. This effect introduces additional modulations to the ARPES spectra (Paggel *et al* 1999, Chiang 2000).

An illuminating ARPES study of QW-states in multilayer graphene films, tracing their transformation from 2D to three-dimensional (3D) character with increase of the film thickness, has been reported by Ohta *et al* (2007). In this work the formation of QW-states was described through multilayer splitting of the π -states coming from each graphene sheet, an approach complementary to the conventional one based on the confinement of delocalized Bloch waves. The ARPES results from this work are reproduced in Fig. 3. The panels (a-d) show the 2D bands near E_F which are formed in a stack of $m = 1 - 4$ graphene layers due to multilayer splitting of the π - and π^* -states from each layer. The corresponding K_z -dependent ARPES response of the π -bands at $E_F - 1$ eV is shown in (e-h). For the monolayer ($m=1$) graphene, an aperiodic $I_{PE}(K_z)$ slowly decaying with $h\nu$ is observed. This reflects,

in accordance with our theoretical picture, the LO-type character of the π^* -state in the single monolayer. As m progressively increases to 4 layers, the π -states split into m pairs of states confined within the stack and, owing to the out-of-plane mirror symmetry of the system, having symmetric $\pm k_z$ values. The corresponding $I_{PE}(K_z)$ evolves to a sequence of peak pairs whose period corresponds to the interlayer distance, exactly the pattern our FT-based formalism predicts for the QC-type states. The peak width progressively decreases with m , reflecting the increase of electron delocalization over the graphene multilayer, expressed by the $E(z)$ -function. With increase of m the individual multilayer-split 2D states form, remarkably, a constellation of peaks whose pattern in the (k_x, K_z) coordinates gradually approaches a K_z -dispersive pattern of ARPES intensity characteristic of the 3D states. This mechanism of the 2D to 3D transformation of the ARPES response, based on the k_z composition of QW-states, is more fundamental compared to the $E(z)$ -only effects (Jovic *et al* 2017, Moser *et al* 2018).

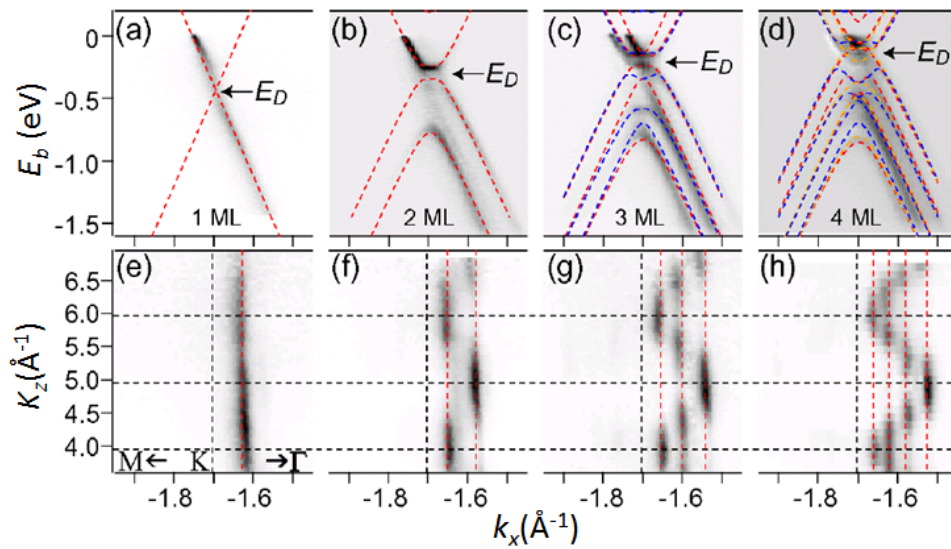


Fig. 3. ARPES data on graphene multilayers: (a-d) The π and π^* -2D bands near E_F for $m = 1 - 4$ graphene layers, respectively. The dashed lines are tight binding calculations; (e-h) Corresponding I_{PE} from the π bands at $E_F - 1\text{eV}$ as a function of (k_x, K_z) . With increase of m these oscillations gradually approach a K_z -dispersive pattern characteristic of the 3D states (adapted from Ohta *et al* 2007).

An impressive example of ARPES applied to QW-states formed in buried heterostructures is the recent study by Lev *et al* (2018) on the GaAlN/GaN interface (for entries on nitride heterostructures see Medjdoub & Iniewski 2015). A large conduction band (CB) offset augmented by strong electric polarization forms at this interface a deep that confines mobile 2D electron gas on the intrinsic GaN side. It typically embeds two QW-states whose Airy-like $E(z)$ -functions, resulting from solution of the model Poisson-Schrödinger equations in the approximately triangular QW, are sketched in Fig. 4(a). The spatial separation of these QW-states from the defect-rich GaAlN barrier layer allows the electrons to escape defect scattering and thereby dramatically increase their mobility. This idea is the fundamental operational principle of so-called high electron mobility transistors (HEMTs) finding their applications in a wide range of microwave devices such as cell phones and radars (Mimura 2002). Because of a relatively large thickness of the GaAlN layer in the operational HEMT heterostructures (in the reported case $\sim 3\text{ nm}$) the buried QW-states can only be accessed with soft-

X-ray ARPES at $h\nu$ above ~ 1000 eV delivering sufficient photoelectron λ (Strocov *et al* 2014). Below we will analyse the ARPES response aspects of the study by Lev *et al* (2018) whereas for its further aspects, including planar anisotropy of electron effective mass propagating into non-linear transport properties of the GaAlN/GaN heterostructures, the reader is referred to the original publication by Lev *et al* (2018).

Fig. 4(b) reproduces the experimental Fermi surface (FS) map of the buried QW-states measured as a function of the in-plane (K_x, K_y) coordinates at $h\nu = 1057$ eV (one of the $I_{PE}(h\nu)$ peaks). The FS appears as tiny electron pockets located at the $\bar{\Gamma}$ -points of the 2D interfacial BZ. As we discussed above, their intensity distribution over different BZs reflects essentially the 2D Fourier series of the QW wavefunctions. The fact of non-vanishing I_{PE} in higher BZs evidences that these wavefunctions embed higher- \mathbf{g} Fourier components coming from the $B(z)$ -part of the QC-wavefunctions, which is beyond their simplistic $E(z)$ -only description. A momentum-distribution curve (MDC) at Fermi energy E_F measured across the $\bar{\Gamma}_{11}$ -point is displayed in (c). Its two external peaks are related to the Fermi momentum k_F^1 of the first QW-state (QWS₁) and two merging internal ones to k_F^2 of the second QW-state (QWS₂) extending deeper into the GaN bulk, as sketched in (b).

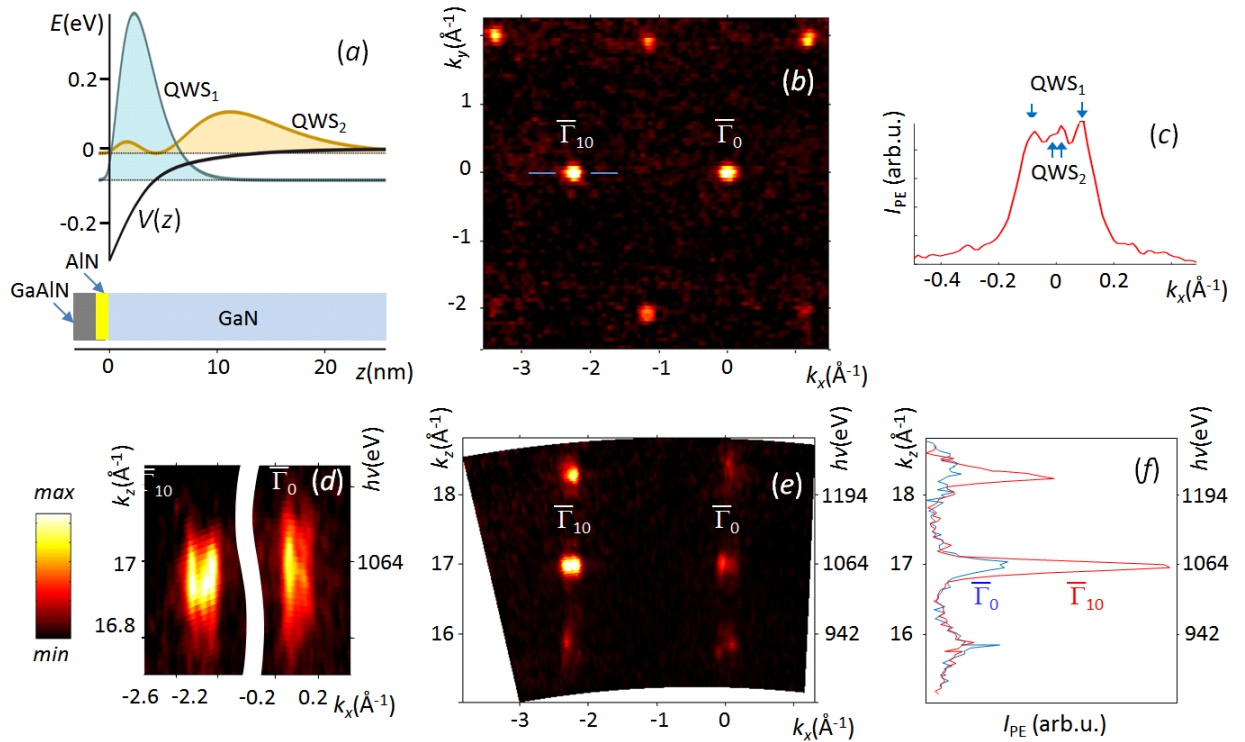


Fig. 4. ARPES data on the buried QW-states in AlGaIn/GaN heterostructure: (a) Model $E(z)$ -function of the two QW-states (top) embedded in the AlGaIn/GaN interface (bottom); (b) Experimental in-plane FS measured at $h\nu = 1057$ eV; (c) MDC at E_F across the $\bar{\Gamma}_{10}$ -point (marked in b) whose peaks identify the two QW-states; (e) Experimental FS cross-section in the $\bar{\Gamma}\bar{M}$ azimuth as a function of K_z and (d) its zoom-in. The 2D character of the QW-states manifests itself in absence of their K_z -dispersion; (f) Fermi intensity in vicinity of the $\bar{\Gamma}_0$ - and $\bar{\Gamma}_{10}$ -points as a function of K_z . The ARPES response peaks coinciding with the integers of G_z confirm that these QW-states are derived from the CBM of bulk GaN in the Γ -point (adapted from Lev *et al* 2018).

Most importantly, Fig. 3(e) reproduces the experimental FS of the QW-states measured in the (K_x, K_z) coordinates. The 2D character of these states manifests itself by the straight FS contours without any K_z -dispersion as emphasized by the zoom-in (d). As predicted by our FT-based theory, the ARPES response $I_{PE}(K_z)$ shows periodic peaks whenever K_z hits the Γ -points (integers of G_z) in the out-of-plane direction. This is particularly clear in the line plots (f) showing Fermi intensity of the two QW-states integrated within $\pm k_F^2$ around the $\bar{\Gamma}_0$ - and $\bar{\Gamma}_{10}$ -points (k_z -separation between the two $\pm k_z$ Bloch-wave components in these QW-states is negligible). Although K_z -width of the $I_{PE}(K_z)$ peaks is limited in this $h\nu$ -range mostly by the final-state Δk_z , in the zoom-in (d) we can distinguish somewhat reduced k_z -width of the QWS₂ compared to QWS₁ which is consistent with the larger spatial extension of the former. Importantly, the K_z -foci of the ARPES peaks coincide with the Γ -points of the bulk BZ. This fact identifies the QW-states in the AlGaIn/GaN heterostructures as originating from the CB minimum (CBM) of the three-dimensional band structure of bulk GaN. In a methodological perspective, such identification can be essential, for example, for studies of valleytronics materials (for entries see Schaibley *et al* 2016) where the CB can include several local minima almost degenerate in energy but separated in \mathbf{k} .

LO-states

ARPES response of the LO-states, aperiodic and decaying with K_z , can be illustrated, for example, by recent results of Weiss *et al* (2015) on a monolayer of perylene tetracarboxylic dianhydride (PTCDA) absorbed on Ag(110). The PTCDA molecular orbitals form LO-type states whose $I_{PE}(K_z)$ is described within the above Fourier-transform formalism. Fig. 5 reproduces the Weiss' *et al* experimental $I_{PE}(h\nu)$ in the central photoemission lobe (points on the graph) for the HOMO and LUMO electron states formed by p_z -orbitals. These dependences are aperiodic and decay with increase of $h\nu$, in agreement with the above theoretical predictions. The zero value of $I_{PE}(h\nu)$ at $K_z = 0$ reflects, as mentioned above, the out-of-plane antisymmetric character of the p_z -orbitals.

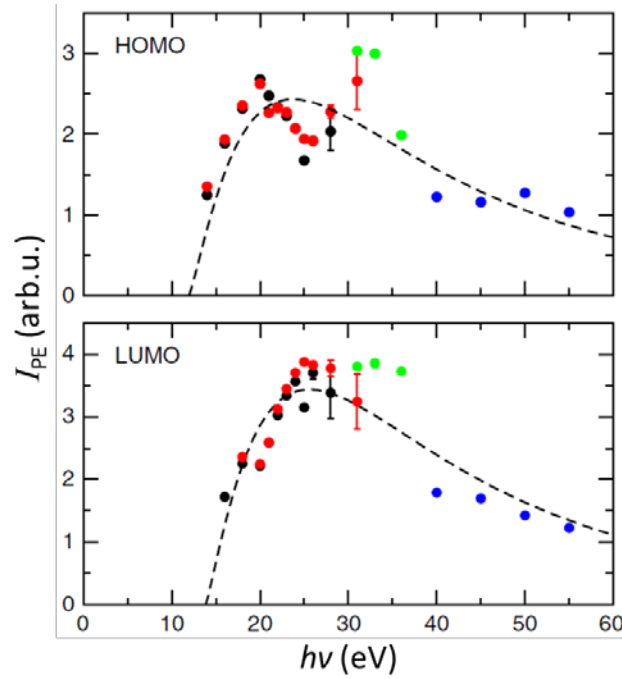


Fig. 5. $h\nu$ -dependent ARPES intensity from the HOMO and LUMO states in a PTCDA molecular monolayer. The aperiodic dependence decaying with increase of $h\nu$ is characteristic of the LO-states. Deviations from predictions of the FE-approximation (dashed lines) are attributed to the shape resonances (adapted from Weiss *et al* 2015).

Deviations of experimental points in Fig. 5 from the smooth trend (dashed lines) expected from FE-description of the final states are attributed to so-called shape resonances. This phenomenon originates from large variations of $V(\mathbf{r})$ at the edges of the adsorbed molecules which distort the ideal FE-wavefront of the final states (Weiss *et al* 2015). We note that 3D-reconstruction of molecular orbitals with ARPES (orbital tomography) can be quite sensitive to such non-FE effects (for a critical review see Bradshaw & Woodruff 2015) because these experiments, restricted by the I_{PE} decay with $h\nu$ and by photo-induced damage of the molecules, typically operate at relatively low energies (below ~ 100 eV) where E_k can be comparable with relatively strong $V(\mathbf{r})$ -variations between the adsorbed molecules and at their interface with the substrate.

Returning to the conventional solid-state systems, the I_{PE} decay with K_z characteristic of the LO-states readily explains, for example, the empirical observation that increase of $h\nu$ clears the ARPES spectra from stray intensity originating, for example, from surface defects left behind by cleavage of the sample (Razzoli *et al* 2012) or introduced by an amorphous overlayer (Woerle 2017).

Conclusion

A lucid Fourier-transform based formalism has been presented that directly relates $h\nu$ -dependent ARPES response of 2D states (surface, interface and QW-states) to Fourier composition and spatial confinement of their wavefunctions. For the QC-type states (including Shockley-Tamm type surface and interface states, and QW-states) formed by out-of-plane periodic Bloch waves modulated by envelope $E(z)$ -functions, the $h\nu$ -dependent ARPES response shows a characteristic pattern of periodic peaks located where photoelectron momentum matches harmonics of the QC-wavefunctions. Amplitudes of the peaks represent the corresponding Fourier series, and their

broadening spatial extension of the $E(z)$ -function. For the LO-type states of purely surface or interface origin (dangling-bond type and defects) the $h\nu$ -dependent ARPES response is described by an aperiodic Voigt-type profile rapidly decaying with $h\nu$, related to spatial localization of these states in the out-of-plane direction. This transparent relation between wavefunctions and their ARPES response enables detailed analysis of different surface, interface and QW-states, as illustrated with ARPES data on the Al(100) surface state, buried interface state in GaAlN/GaN heterostructures, molecular orbitals of PTCDA, etc. This analysis is particularly accurate in the soft-X-ray energy range where the final states are close to pure plane waves with small intrinsic out-of-plane momentum broadening. The developed methodology paves ways towards experimental analysis and design of 2D wavefunctions in real electronic devices.

Acknowledgements

I thank E. E. Krasovskii for sharing theoretical concepts and critical reading of the manuscript, J. H. Dil for insightful discussions, and L. L. Lev for promoting scientific exchange and help with the GaAlN/GaN data processing. The permissions of P. Hofmann, E. Rotenberg and P. Puschnig to reproduce their impressive results are gratefully acknowledged.

References

- P. Borghetti, J. Lobo-Checa, E. Goiri, A. Mugarza, F. Schiller, J. E. Ortega & E.E. Krasovskii. *Effect of surface reconstruction on the photoemission cross-section of the Au(111) surface state*. J. Phys.: Condens. Matter **24** (2012) 395006
- A M Bradshaw & D P Woodruff, *Molecular orbital tomography for adsorbed molecules: is a correct description of the final state really unimportant?* New J. Phys. **17** (2015) 013033
- M. Bianchi, D. Guan, S. Bao, J. Mi, B.B. Iversen, P.D. King & P. Hofmann. *Coexistence of the topological state and a two-dimensional electron gas on the surface of Bi₂Se₃*. Nat. Commun. **1** (2010) 128
- J. Braun & M. Donath. *Theory of photoemission from surfaces*. J. Phys.: Condens. Matter **16** (2004) S2539
- C. Cancellieri, A. S. Mishchenko, U. Aschauer, A. Filippetti, C. Faber, O. S. Barišić, V. A. Rogalev, T. Schmitt, N. Nagaosa & V. N. Strocov. *Polaronic metal state at the LaAlO₃/SrTiO₃ interface*. Nat. Commun. **7** (2016) 10386.
- T.-C. Chiang. *Photoemission studies of quantum well states in thin films*. Surf. Sci. Rep. **39** (2000) 181
- P. H. Dederichs. *Dynamical Diffraction Theory by Optical Potential Methods*. Solid State Physics **27** (1972) eds. H. Ehrenreich, F. Seitz & D. Turnbull (New York: Academic) p. 136
- L. Colakerol, L. Piper, A. Fedorov, T. Chen, T. Moustakas & K. Smith. *Potassium and ion beam induced electron accumulation in InN*. Surf. Sci. **632** (2015) 154
- P. J. Feibelman & D. E. Eastman. *Photoemission spectroscopy – Correspondence between quantum theory and experimental phenomenology*. Phys. Rev. B **10**, 4932 (1974)
- V. Heine. *On the General Theory of Surface States and Scattering of Electrons in Solids*. Proc. Phys. Soc. **81** (1963) 300
- Ph. Hofmann, Ch. Soendergaard, S. Agergaard, S. V. Hofmann, J. E. Gayone, G. Zampieri, S. Lizzit & A. Baraldi. *Unexpected surface sensitivity at high energies in angle-resolved photoemission*. Phys. Rev. B **66** (2002) 245422
- J. E. Inglesfield. *Surface electronic structure*. Rep. Prog. Phys. **45** (1982) 223
- J. Jiang, Z. Liu, Y. Sun, H. Yang, C. Rajamathi, Y. Qi, L. Yang, C. Chen, H. Peng, C.-C. Hwang, S. Sun, S.-K. Mo, I. Vobornik, J. Fujii, S. Parkin, C. Felser, B. Yan & Y. Chen. *Signature of type-II Weyl semimetal phase in MoTe₂*. Nat. Commun. **8** (2017) 13973.
- V. Jovic, S. Moser, S. Ulstrup, D. Goodacre, E. Dimakis, R. Koch, G. Katsoukis, L. Moreschini, S.-K. Mo, C. Jozwiak, A. Bostwick, E. Rotenberg, T. D. Moustakas & K. E. Smith, *How Indium Nitride Senses Water*. Nano Letters **17** (7339) 2017
- S. D. Kevan, N. G. Stoffel & N. V. Smith. *High-resolution angle-resolved photoemission studies of the surface states on Al(111) and Al(001)*. Phys. Rev. B **31** (1985) 1788; Surface states on low-Miller-index copper surfaces. Phys. Rev. B **31** (1985) 3348
- P. Kluuiev, T. Latychevskaia, J. Osterwalder, M. Hengsberger & L. Castiglioni. *Application of iterative phase-retrieval algorithms to ARPES orbital tomography*. New J. Phys. **18** (2016) 093041
- E. E. Krasovskii & W. Schattke. *Angle-resolved photoemission from surface states*. Phys. Rev. Lett. **93** (2004) 027601

- E.E. Krasovskii, V.N. Strocov, N. Barrett, H. Berger, W. Schattke & R. Claessen. *Band mapping in the one-step photoemission theory: Multi-Bloch-wave structure of final states and interference effects*. Phys. Rev. B **75**, 045432 (2007)
- E. E. Krasovskii, W. Schattke, P. Jiříček, M. Vondráček, O. V. Krasovska, V. N. Antonov, A. P. Shpak & I. Bartoš. *Photoemission from Al(100) and (111): Experiment and ab initio theory*. Phys. Rev. B **78** (2008) 165406
- G. Landolt, S. V. Eremeev, Y. M. Koroteev, B. Slomski, S. Muff, T. Neupert, M. Kobayashi, V. N. Strocov, T. Schmitt, Z. S. Aliev, M. B. Babanly, I.R. Amiraslanov, E. V. Chulkov, J Osterwalder & J. H. Dil. *Disentanglement of Surface and Bulk Rashba Spin Splittings in Noncentrosymmetric BiTeI*. Phys. Rev. Lett. **109** (2012) 116403
- L. L. Lev, I. O. Maiboroda, M.-A. Husanu, E. S. Grichuk, N. K. Chumakov, I. S. Ezubchenko, I. A. Chernych, X.Wang, B. Tobler, T. Schmitt, M. L. Zhanavskiy, V. G. Valeev & V. N. Strocov. *k-space imaging of anisotropic 2D electron gas in GaN/GaN high-electron-mobility transistor heterostructures*. Nature Comm. **9** (2018) 2653
- S. G. Louie, P. Thiry, R. Pinchaux, Y. Pétroff, D. Chandesris & J. Lecante. *Periodic Oscillations of the Frequency-Dependent Photoelectric Cross Sections of Surface States: Theory and Experiment*. Phys. Rev. Lett. **44** (1980) 549
- G. Mahan. *Theory of photoemission in simple metals*. Phys. Rev. B **2** (1970) 4334
- F. Medjdoub & K. Iniewski (eds.) *Gallium Nitride (GaN): Physics, Devices, and Technology*. CRC Press (2015).
- T. Mimura. *The early history of the high electron mobility transistor (HEMT)*. IEEE Trans. Microw. Theory Techn. **50** (2002) 780
- M. Milun, P. Pervan & D.P. Woodruff. *Quantum well structures in thin metal films: simple model physics in reality?* Rep. Prog. Phys. **65** (2002) 99
- T. Miller, A. Samsavar & T.-C. Chiang. *Photoexcitation of resonances in Ag films on Ni(111)*. Phys. Rev. B **50** (1994) 17686
- J. A. Miwa, P. Hofmann, M. Y. Simmons & J. W. Wells. *Direct Measurement of the Band Structure of a Buried Two-Dimensional Electron Gas*. Phys. Rev. Lett. **110** (2013) 136801
- S. Moser. *An experimentalist's guide to the matrix element in angle resolved photoemission*. J. Electron Spectr. Relat. Phenom. **225** (2017) 29
- S. Moser, V. Jovic, R. Koch, L. Moreschini, J.-S. Oh, C. Jozwiak, A. Bostwick & E. Rotenberg. *How to extract the surface potential profile from the ARPES signature of a 2DEG*. J. Electron Spectr. Relat. Phenom. **225** (2018) 16
- A. Mugarza, J.E. Ortega, A. Mascaraque, E.G. Michel, K.N. Altmann & F.J. Himpsel. *Periodicity and thickness effects in the cross section of quantum well states*. Phys. Rev. B **62** (2000) 12672
- A. Mugarza, J.E. Ortega, A. Mascaraque, E.G. Michel, K.N. Altmann, F.J. Himpsel. *Probing unoccupied bulk bands via the cross section of quantum well states in thin films*. Surf. Sci. **482-485** (2001) 464
- T. Ohta, A. Bostwick, J. L. McChesney, T. Seyller, K. Horn & E. Rotenberg. *Interlayer Interaction and Electronic Screening in Multilayer Graphene Investigated with Angle-Resolved Photoemission Spectroscopy*. Phys. Rev. Lett. **98** (2007) 206802

- J. E. Ortega, F. J. Himpsel, G. J. Mankey & R. F. Willis. *Quantum-well states and magnetic coupling between ferromagnets through a noble-metal layer*. Phys. Rev. B **47** (1993) 1540
- J.J. Paggel, T. Miller, T.-C. Chiang. *Angle-resolved photoemission from atomic-layer-resolved quantum well states in Ag/Fe(100)*. J. Electron Spectrosc. Relat. Phenom. **101-103** (1999) 271.
- C. J. Powell, A. Jablonski, I. S. Tilinin, S. Tanuma & D. R. Penn. *Surface sensitivity of Auger-electron spectroscopy & X-ray photoelectron spectroscopy*. J. Electron Spectrosc. Relat. Phenom. **98/99** (1999) 1
- P. Puschnig, S. Berkebille, A. J. Fleming, G. Koller, K. Emtsev, T. Seyller, J. D. Riley, C. Ambrosch-Draxl, F. P. Netzer & M. G. Ramsey. *Reconstruction of molecular orbital densities from photoemission data*. Science **326** (2009) 702
- E. Razzoli, M. Kobayashi, V. N. Strocov, B. Delley, Z. Bukowski, J. Karpinski, N.C. Plumb, M. Radović, J. Chang, T. Schmitt, L. Patthey, J. Mesot & M. Shi. *Bulk Electronic Structure of Superconducting LaRu₂P₂ Single Crystals Measured by Soft-X-Ray Angle-Resolved Photoemission Spectroscopy*. Phys. Rev. Lett. **108** (2012) 257005
- M.G. Reuter. *A unified perspective of complex band structure: interpretations, formulations and applications*. J. Phys.: Condens. Matter **29** (2017) 053001
- J. R. Schaibley, H. Yu, G. Clark, P. Rivera, J. S. Ross, K. L. Seyler, W. Yao & X. Xu. *Valleytronics in 2D materials*. Nat. Rev. Mater. **1**, 16055 (2016).
- V. N. Strocov, H. Starnberg & P. O. Nilsson. *Excited-state b&s of Cu determined by VLEED b& fitting & their implications for photoemission*. Phys. Rev. B **56** (1997) 1717
- V. N. Strocov, H. I. Starnberg, P. O. Nilsson, H. E. Brauer & L.J. Holleboom. *New method for absolute b& structure determination by combining photoemission with Very-Low-Energy Electron Diffraction: Application to Layered VSe₂*. Phys. Rev. Lett. **79** (1997) 467
- V. N. Strocov. *Intrinsic accuracy in 3-dimensional photoemission band mapping*. J. Electron Spectrosc. Relat. Phenom. **130** (2003) 65
- V.N. Strocov, E.E. Krasovskii, W. Schattke, N. Barrett, H. Berger, D. Schrupp & R. Claessen. *Three-dimensional b& structure of layered TiTe₂: Photoemission final-state effects*. Phys. Rev. B **74** (2006) 195125
- V. N. Strocov, M. Shi, M. Kobayashi, C. Monney, X. Wang, J. Krempasky, T. Schmitt, L. Patthey, H. Berger & P. Blaha. *Three-Dimensional Electron Realm in VSe₂ by Soft-X-Ray Photoelectron Spectroscopy: Origin of Charge-Density Waves*. Phys. Rev. Lett. **109** (2012) 086401
- V. N. Strocov, M. Kobayashi, X. Wang, L. L. Lev, J. Krempasky, V. A. Rogalev, T. Schmitt, C. Cancellieri & M. L. Reinle-Schmitt. *Soft-X-ray ARPES at the Swiss Light Source: From 3D Materials to Buried Interfaces & Impurities*. Synchrotron Radiat. News **27** (2014) 31
- S. Suga & Ch. Tusche, *Photoelectron spectroscopy in a wide hv region from 6 eV to 8 keV with full momentum & spin resolution*. J. Electron Spectr. Relat. Phenom. **200** (2015) 119
- S. Weiss, D. Lüftner, T. Ules, E. M. Reinisch, H. Kaser, A. Gottwald, M. Richter, S. Soubatch, G. Koller, M. G. Ramsey, F. S. Tautz & P. Puschnig, *Exploring three-dimensional orbital imaging with energy-dependent photoemission tomography*. Nature Comm. **6** (2015) 8287

J. Woerle, F. Bisti, M.-A. Husanu, V. N. Strocov, C. W. Schneider, H. Sigg, J. Gobrecht, U. Grossner & M. Camarda. Electronic *band structure of the buried SiO₂/SiC interface investigated by soft x-ray ARPES*. Appl. Phys. Lett. **110** (2017) 132101

K. Yoshimatsu, K. Horiba, H. Kumigashira, T. Yoshida, A. Fujimori, M. Oshima. *Metallic Quantum Well States in Artificial Structures of Strongly Correlated Oxide*. Science **333** (2011) 319